EUROFUSION WPJET1-PR(16) 14950

VA Yavorskij et al.

Fokker-Planck model for collisional loss of fast ions in tokamaks

Preprint of Paper to be submitted for publication in
Nuclear Fusion

This work has been carried out within the framework of the EUROfusion Consortium and has received funding from the Euratom research and training programme 2014-2018 under grant agreement No 633053. The views and opinions expressed herein do not necessarily reflect those of the European Commission.

Fokker-Planck model for collisional loss of fast ions in tokamaks

V. Yavorskij[1,2], V. Goloborod'ko[1,2], K. Schoepf[1]

[1]*Institute for Theoretical Physics, University of Innsbruck, Austria*
[2]*Institute for Nuclear Research, Ukrainian Academy of Sciences, Kyiv, Ukraine*
Email: Victor.Yavorskij@uibk.ac.at

ABSTRACT

Modelling of the collisional loss of fast ions from tokamak plasmas is important from the point of view of the impact of fusion alphas and NBI ions on plasma facing components as well as for the development of diagnostics of fast ion losses [1-3]. The present paper develops a 4D Fokker-Planck approach for the assessment of distributions of collisional loss of fast ions as depending on the coordinates of the first wall surface and on the velocities of lost ions. Based on this newly developed Fokker-Planck approach the poloidal distribution of neoclassical loss of fast ions from tokamak plasma may be examined as well as the contribution of this loss as dependent on pitch-angle and energy to the signal detected by the scintillator probe may be evaluated. It is pointed out that the loss distributions obtained with the novel Fokker-Planck treatment will be useful for the verification of Monte-Carlo models [4, 5] used for simulating fast ion loss from toroidal plasmas.

PACS numbers: 52.55.Fa, 52.55.Pi, 52.65.Cc, 52.65.Ff, 52.65.Pp

1. Introduction

Precise modelling of the fast ion fluxes onto the plasma facing components (SPFC) in tokamaks is important for predicting the heat load and fluences associated with charged fusion products and beam ions escaping from the confining magnetic configuration in future fusion reactors. Further, such modelling enables the identification and interpretation of the loss mechanisms of fast ions in present day tokamak plasmas [1, 6, 7]. Typically, relevant simulations were based on Monte-Carlo approaches [4, 5] or on simplified models of poloidal distributions only [8, 9] and provide a qualitative rather than quantitative information on loss distributions. Former Fokker-Planck treatments of the radial fluxes of fast ions from the tokamak plasmas [9, 10] were carried out supposing the simplified shape of the first wall and neglecting the effects of gyro motion.

A detailed predictive modelling of fast ion loss distributions requires the development of new approaches or at least a substantial improvement of the existing methods [4, 5, 9, 10]. The purpose of the present paper is to establish a technique for assessing the distributions of energetic ion loss induced by the Coulomb collisions in tokamaks using the Fokker-Planck (FP) approach. The paper extends former Fokker-Planck treatments of the poloidal distributions of fast ion loss induced by Coulomb collisions [11, 12] to an arbitrary poloidal shape of the first wall and accounts for the effects of finite gyro radius. It focuses on the

losses due to collision induced radial transport of fast ions. It should be pointed out that radial transport associated with Coulomb collisions is expected to determine the losses of energetic charged fusion products in ITER [13].

2. Fokker-Planck equation in the constant-of-motion space

Our study is based on the drift FP equation for fast ions in the phase space of motion invariants, $\boldsymbol{c}$, and of angular coordinates, $\boldsymbol{\theta}$, determining the particle position on the orbit. In case of axisymmetric tokamak considered here such a position is specified by the poloidal angular coordinate, ϑ, only. Therefore, it is sufficient to employ the FP treatment in a 4D phase space $\mathbf{x}=\{\boldsymbol{c},\vartheta\}$, i.e.

$$\partial_t f + \dot{\vartheta}\partial_\vartheta f = L_{\mathbf{x}} f + S(\mathbf{x}), \quad L_{\mathbf{x}} = \nabla_{\mathbf{x}} \cdot \left(\mathbf{d}_{\mathbf{x}} - \ddot{\mathbf{D}}_{\mathbf{x}} \cdot \nabla_{\mathbf{x}}\right) \tag{1}$$

where $\mathbf{d}_{\mathbf{x}}$ and $\ddot{\mathbf{D}}_{\mathbf{x}}$ describe convective and diffusive collisional transport of fast ions associated correspondingly with the slowing down, pitch-angle scattering and diffusion in energy and S($\mathbf{x}$) is the source term. We also suppose that fast ions are a weak component (number and and energy density small compared with background) of plasma [14].

2.1 <u>FP description of confined ions</u> Due to the smallness of the collisional rates of the slowing down, ν_s, of the pitch-angle scattering, $\nu_\perp$, and of diffusion in energy, $\nu_\parallel$, as compared to the frequency of poloidal motion, $\dot{\vartheta}$, the distribution function of confined ions, $f(\mathbf{x})$, can be represented as a superposition of the dominant part, $f_0(\boldsymbol{c})$, which is independent on angular coordinate and of a small oscillating part, $f_1(\boldsymbol{c},\vartheta)$, varying periodically with ϑ. Note that $f_0(\boldsymbol{c})$ satisfactorily describes the ions with confined orbits and is determined by bounce averaged FP equation in 3D constant-of-motion (COM) space [9, 10]

$$\partial_t f_0 = \langle L_{\mathbf{x}} \rangle f_0 + \langle S \rangle, \quad \langle ... \rangle = \oint d\vartheta \sqrt{g_{\mathbf{x}}}\,(...) \equiv \Omega(\mathbf{c}) \oint d\vartheta (...)/\dot{\vartheta} \tag{2}$$

where $\sqrt{g_{\mathbf{x}}}$ is the Jacobian of transformation from Eulerian coordinates ($\mathbf{r}$,$\mathbf{v}$) to Lagrangian coordinates $\mathbf{x}$, $\Omega \equiv \sqrt{g_{\mathbf{x}}}\dot{\vartheta}$ is ϑ-independent value due to an evident relationship $\nabla_{\mathbf{x}} \cdot \dot{\mathbf{x}} = 0$. Distribution function $f_0(\boldsymbol{c})$ can be obtained by solving a boundary value problem in the COM space. Following [9, 10] we can use the following set of COM variables: energy E, normalised magnetic moment λ and radial coordinate R_{m} denoting the maximum major radius R along the guiding centre orbit for trapped and co-passing particles and the minimum major

radius along the guiding centre orbit for counter-passing particles. In case of up-down symmetric (or only slightly asymmetric) magnetic configuration the values of $R=R_m$ are reached at the plasma equatorial plane, $Z=Z_{eq}$. Evidently that owing to the axisymmetric limit accepted here the shape of 3D **c**-domain of fast ions confined in the absence of collisions is determined both by the parameters of magnetic configuration and by the poloidal shape of the plasma facing surface. Fig. 1 demonstrates the typical shape of the confinement domain in the plane spanned by the COM variables R_m and $\xi_m=V_{\|}(R=R_m, Z=Z_{eq}, \lambda)/V$ at fixed energy for the JET-like magnetic configuration. To inspect the confinement domain boundaries in Fig. 1 we have supposed the parabolic profiles of the safety factor, $q=q_0+(q_a-q_0)x^2$, and of the Shafranov shift, $\Delta=\Delta_0(1-x^2)$, with x - the normalised flux surface radius [15], $q_a/q_0=5/1$ and $\Delta_0=0.15$m. The flux surfaces are assumed to be up-down symmetric with elongation k=1.7. Furthermore we have supposed the axisymmetric plasma facing surface with the poloidal shape $R=W(Z)$ corresponding to the shape of inner surface of poloidal limiters at least in the vicinity of plasma equatorial plane. At the above assumptions the confinement condition for co-passing and trapped ions can be represented as $R_m<R_{mLBS}=W_{LBS}(Z_{eq})/(1+\rho\sin\zeta_m/R_c)$, where $\rho=V/\omega_c$, $V=(2E/m)^{1/2}$ – ion velocity, $\omega_c=eB_c/(mc)$ – gyro frequency at $R=R_c=2.86m$, $W_{LBS}(Z_{eq})=3.9m$ and ζ_m pitch angle at $R=R_m$, $Z=Z_{eq}$. Respectively for ctr-passing ions the confinement condition has a form $R_m> R_{mHBS}=W_{HBS}(Z_{eq})/(1+\rho_c\sin\zeta_m/R_c)$ with $W_{HBS}(Z_{eq})=1.82m$.

It is clearly seen in Fig. 1 that the confinement domain of ctr-passing ions is well separated from the domain of co-passing and trapped ions both in R_m and in ξ_m variables. The counter-passing ions are entirely localised at the high-B side of the plasma (at R less than the magnetic axis major radius R_{ax}) while the co-passing and trapped ions are located completely at $R>R_{ax}$. The collisional exchange between ions from the left domain and ions from the right domain is possible only through the trapped/passing separatrix represented by the ctr-circulating/trapped boundary (red solid line) and by the trapped/ctr-circulating boundary (red broken line). Both domains are partially bounded by well confined ions executing the stagnation (violate lines) and strictly ctr(co)-passing (green lines) orbits. Fast ions can be lost to the wall via the radial diffusion through the boundaries represented by the marginaly confined orbits (violate broken lines at R_m close to $R_{wHBS}=1.82m$ for ctr-passing domain and at R_m close to $R_{wLBS}=3.9m$ for co-passing and trapped particle domain). Finally ctr-passing ions with $\rho=5cm$ can be lost due to the scattering of marginally confined ctr-passing ions into the unconfined orbits of barely trapped ions through the loss-cone boundary (red broken line).

Typical orbits of ions lost as a result of radial diffusion and due to scattering into the loss-cone are shown in Fig. 2.

Note that the shape of confinement domain in R_m, ξ_m variables is extremely sensitive to the energy of fast ions. This is obviously demonstrated by Fig. 3 displaying the λ=0 slice of 3D **c**-domain of confined fast ions. Shown in this figure is also the area of trapped orbits, areas with possible collisional exchange between the ctr-passing and trapped orbits as well as areas of marginally confined orbits and of ctr-passing orbits scattered into loss-cone. It is seen also that depending on ion energy one should distinguish between the 5 ranges with qualitatively different orbit topology of confined fast ions and with different loss mechanisms. We note that co-passing ions are better confined as compared to the ctr-passing ones. This is confirmed by Fig. 4 where displayed are the confinement domains of ctr- and co-passing ions in R_m, ξ_m variables at high energies (ρ = 20*cm*, 31*cm* and 40*cm*). It is seen that at high-energy confined are only ions with nearly stagnation orbits at small $V_\perp$. The reason of substantial dissimilarity in the maximum energy of confined ctr-passing ($\rho_4 \cong$ 32cm) and co-passing fast ions ($\rho_5 \cong$ 46cm) is the Shafranov shift enhancing the B_Z component of poloidal magnetic field at $R>R_{ax}$ and correspondingly allowing for the stagnation condition at higher energies.

Table 1 Energy ranges (see Fig. 3) with different orbit topology and confinement properties of fast ions

Energy range	Main features		
	ctr-passing (p^-)	trapped (t)	co-passing (p^+)
$\rho<\rho_1$	p^-t exchange Radial diffusion (RD) loss Cone loss	tp^- exchange tp^+ exchange RD loss	p^+t exchange RD loss
$\rho_1<\rho<\rho_2$	RD loss Cone loss	tp^+ exchange RD loss	p^+t exchange RD loss
$\rho_2<\rho<\rho_3$	RD loss Cone loss		RD loss
$\rho_3<\rho<\rho_4$	Cone loss		RD loss
$\rho_4<\rho<\rho_5$			RD loss

Evidently that, in the case of confined orbits, R_m cannot exceed the value of $R_{mLBS}(E, \xi_m)$ corresponding to the marginally confined orbits of co-passing and trapped ions. Analogously the R_m should exceed the $R_{mHBS}(E, \xi_m)$ – the R_m-boundary of the confinement domain of ctr-passing ions. Moreover $f_0(\mathbf{c})$ should satisfy the following boundary condition

$$f_0\left(E,\xi_m,R_{\rm m}=R_{\rm mMCO}\right)=0,\quad R_{\rm mMCO}=\begin{cases}R_{\rm mLBS}\left(E,\xi_m\right)\ \text{if}\ \xi_m\geq 0\\ R_{\rm mHBS}\left(E,\xi_m\right)\ \text{if}\ \xi_m\leq 0\end{cases}. \tag{3}$$

In addition $f_0(\mathbf{c})$=0 at the boundary of ctr-passing ions with unstable stagnation orbits corresponding to loss cone. Knowledge of the $f_0(\mathbf{c})$ allows to find the oscillating part of distribution function $f_1(\mathbf{c},\vartheta)$ by performing the ϑ-integration of Eq. (1), i.e.

$$\Omega f_1=\widehat{L}_{\mathbf{x}}f_0+\widehat{S}\left(\mathbf{x}\right),\quad (...)=\int_0^{\vartheta}d\vartheta\sqrt{g_{\mathbf{x}}}\,(...), \tag{4}$$

where poloidal variable ϑ is determined by the relationship

$$r=r_{\max}\left(\mathbf{c}\right)-\left[r_{\max}\left(\mathbf{c}\right)-r_{\min}\left(\mathbf{c}\right)\right]\sin^2\frac{\vartheta}{2},\quad 0\leq\vartheta<2\pi \tag{5}$$

with r the flux surface radius, r_{max} and r_{min} the maximum and minimum radial coordinate on the particle orbit. An explicit expression for $\widehat{L}_{\mathbf{x}}$ in ($\boldsymbol{c},\vartheta$) variables is presented in Appendix 1. Note that generally the oscillating part of distribution function $f_1\left(\vartheta;E,\xi_m,R_{\rm m}=R_{mMCO}\right)\neq 0$ and is dominant for marginally confined ions with $R_{\rm m}\to R_{\rm mMCO}$. Evidently that the radial flux of fast ions lost to the first wall is determined by those with the unconfined orbits, i.e. with $R_{\rm m} > R_{\rm mLBS}$ for co-passing and trapped ions and with $R_{\rm m} < R_{\rm mHBS}$ for ctr-passing ions.

2.2 <u>FP description of unconfined ions</u> To examine the distribution function of lost ions we use a set of COM variables $\hat{\mathbf{c}}=\left\{E,\xi_l,Z_l\right\}$, where ξ_l and Z_l are pitch-angle cosine and poloidal coordinate at the first wall (see Fig. 5). To account for the finite gyroradius effects on the distribution function of escaping ions we will suppose that particle is lost when the distance between the guiding centre and the PFS is equal to the gyro-radius value. Under this assumption the guiding centre coordinates R_{gl} and Z_{gl} of the particle lost onto the axisymmetric plasma facing surface with the poloidal shape $R=W(Z)$ can be represented in the following form

$$\begin{aligned}&R_{gl}=\frac{W\left(Z_l\right)}{1+\dfrac{\sigma_l\rho\sin\zeta_l}{R_c\sqrt{1+W'^2\left(Z_l\right)}}},\quad Z_{gl}=Z_l+\frac{W'\left(Z_l\right)W\left(Z_l\right)\sigma_w\rho\sin\zeta_l}{R_c\sqrt{1+W'^2\left(Z_l\right)}+\sigma_l\rho\sin\zeta_l}\\ &\rho=\frac{V}{\omega_c},\quad \xi_l=\cos\zeta_w,\sin\zeta_l=\frac{V_{\perp l}}{V},\quad \sigma_l=sign\left(V_{\|l}\right)\end{aligned}. \tag{6}$$

Expressions (6) for R_{gl} and Z_{gl} are valid only for particles at the moment when the full orbits are tangent to the PFS, namely at the moment when the normal to the PFS component of velocity of lost particle $V_n(Z_l)$ = 0. In reality the lost orbits are not unavoidably tangent to PFS

and particle can be lost when $V_n(Z_l)>0$ and when the guiding centre of lost particle is located slightly closer to the PFS than the gyroroadius [16]. This is demonstrated by Fig. 6 where compared are orbits with $V_n=0$ and $V_n>0$. However according to Fig. 6 (see also [16]) we conclude that the difference between the guiding centre positions for particle lost at Z_l with given V and ξ_l but with different V_n is very small (<< gyro radius). Consequently in our analytical treatment we suppose that relationships (6) providing $R_{gl}(\xi_l, Z_l)$, $Z_{gl}(\xi_l, Z_l)$ are valid for all lost ions. Similarly to confined poloidal variable ϑ for confined orbits, the cyclic poloidal variable $\hat{\vartheta}$ for unconfined ones is determined by the relationship

$$\begin{aligned} r &= r_{gl}\left(R_{gl}, Z_{gl}\right) - \Delta \sin^2 \frac{\hat{\vartheta}}{2}, \quad 0 \le \vartheta < 2\pi \\ \Delta &= r_{gl} - r_{\min}\left(V, \xi_l, Z_l\right) \end{aligned} \tag{7}$$

where r_{gl} is a flux surface radius of a guiding centre at $R=R_{gl}(\xi_l, Z_l)$, $Z=Z_{gl}(\xi_l, Z_l)$. In present study the fast ions, escaping to the first wall as a result of collisional convection and diffusion transport, are described by 4D FP equation (1) in variables $\hat{x} = \left\{\hat{c}, \hat{\vartheta}\right\} \equiv \left\{E, \xi_l, \chi_l; \hat{\vartheta}\right\}$. An explicit expression for $L_{\hat{\mathbf{x}}}$ is presented in Appendix 2. It is important that diffusion and convection in poloidal coordinate Z_l significantly dominate those in pitch angle ξ_l as well as in the energy. The reason for that is localisation of lost particles in rather narrow range of poloidal angles [8, 12], $\Delta\chi \sim 0.1 - 0.3 << \pi$, where

$$\Delta\chi = \left(\frac{4 D_r \tau_b}{a^2} \frac{V_\chi^2}{V_d^2} \right)^{1/4}, \tag{8}$$

D_r is the radial diffusion coefficient of lost ions; V_χ and V_d are correspondingly poloidal and drift components of particle velocity, a the plasma radius and τ_b the bounce period. Domination of convective and diffusive transport in poloidal coordinate $\hat{x}^3 \equiv Z_l$ makes possible to neglect the collisional fluxes in $\hat{x}^2 \equiv \xi_l$ and in $\hat{x}^1 \equiv E$ and to use a reduced 2D FP equation of a following form (see Appendix 2)

$$\hat{\Omega}\left(\mathbf{c}_l\right) \partial_{\hat{\vartheta}} f = \partial_{Z_l} \sqrt{g_{\mathbf{c}_l \hat{\vartheta}}} \left(d^3_{\mathbf{c}_l \hat{\vartheta}} - D^{33}_{\mathbf{c}_l \hat{\vartheta}} \partial_{Z_l} \right) f . \tag{9}$$

Source term $S\left(\hat{\mathbf{x}}\right)$ is not accounted for in Eq. (9) because in the case of unconfined ions it is associated with the collisionless first orbit losses and not with the collisional convective and diffusive ones. Finally Eq. (9) should be appended by the following initial and boundary conditions

$$f\left(\hat{\vartheta}, Z_l; E, \xi_l\right)\Big|_{\hat{\vartheta}=0} = 0,$$
$$f\left(\hat{\vartheta}, Z_l; E, \xi_l\right)\Big|_{\chi_{\mathrm{fw}}=0} = f_1\left[E, \xi_m = \xi_l, R_m = R_{gl}\left(Z_l = Z_{eq}; E, \xi_l\right); \hat{\vartheta} = \vartheta\right]. \quad (10)$$

In Eq. (10) the function $f_1\left[E, \xi_m = \xi_l, R_m = R_{gl}\left(Z_l = Z_{eq}; E, \xi_l\right); \hat{\vartheta} = \vartheta\right]$ is determined by Eq. (2) and corresponds to the marginally confined fast ion, variables $\{E, \xi_l\}$ in present 2D FP treatment are the parameters.

Radial flux $\Gamma\left(E, \xi_l, \chi_l\right)$ of fast ions lost to the first wall is determined by the following expression

$$\Gamma\left(\chi_l, E, \xi_l\right) = f\left(\hat{\vartheta} = 2\pi, Z_l; E, \xi_l\right) V_d^r\left(Z_l, E, \xi_l\right), \quad (11)$$

where V_d^r is the particle radial velocity at the first wall. Thus solution of Eq. (9) under conditions (10) allows examination of spatial and velocity distributions of collisional loss via simple formula (11).

2.3 <u>Results of numerical modeling</u> Here we represent the results of numerical evaluation of the poloidal and pitch-angle distributions of a convective-diffusive collisional loss of 130 *keV* deuterons to the first wall of JET-like tokamak plasma with a = 0.95 *m* and R_c = 2.95 *m*, $n_e(0) = n_i(0) = 0.7\cdot10^{14}$ m^{-3}, $n_e(a) = n_i(a) = 0.2\cdot10^{14}$ m^{-3}, $T_e(0) = T_i(0)$ = 5.0 *keV*, $T_e(a) = T_i(a)$ = 1.0 *keV*. We use also model magnetic configuration with Shafranov shift 0.2 *m*, elongation $k(0)$ = 1.3, $k(a)$ = 1.7, triangularity = 0.15 and plasma current I = 2.5*MA*. To simplify simulation we suppose that $f_1\left(E, \lambda, r_{\max} = a; \vartheta\right) \propto \sin\left(\vartheta/2\right)$. Fig. 7 displays the calculated distribution function of lost 130 *keV* deuterons with pitch-angle cosine ξ_l=0.5 as dependent on the polidal angular variable $\hat{\vartheta}$ and poloidal coordinate at the wall Z_l. As expected, $f(\hat{\vartheta}, Z_l)$ is localised in rather narrow range of Z below the mid-plane $-0.2m < Z_l < 0.3m$. Fig. 8 represents the distribution of lost co-circulating deuterons over the pitch angle cosine ξ_l and poloidal coordinate Z_l at the first wall. The maximum loss is observed at Z_l = 0.1*m* for marginally trapped ions with ξ_l = 0.65.

3. Conclusions

We demonstrate that in drift approximation the distribution function of fast ions lost from the axisymmetric tokamak plasmas as a result of collisional convection-diffusion transport can be treated by 1D in COM space and 1D in poloidal angular coordinate Fokker-Planck kinetic equation. Solution of this equation allows direct evaluation of the spatial and velocity distributions of the flux of lost ions to the tokamak first wall. Modeled collisional loss of fast deuterons in JET-like tokamak are found to be localized in rather narrow range of poloidal coordinate Z ($-0.2m < Z < 0.3m$) below the plasma midplane. It should be pointed out that solution of the boundary value problem for lost fast ions allows to extend our Fokker-Planck code FIDIT [9, 11] oriented at present time predominantly on the description of confined fast ions (only velocity distributions of total loss of fast ions are calculated) also to detailed description of lost ions (including loss distribution over the tokamak first wall). Finally we note that approach developed accounts for effects of gyro motion and real poloidal shape of plasma facing surface and should be useful for the verification of Monte-Carlo models used for the simulation of fast ion loss from toroidal plasmas as well.

Acknowledgement

This work has been carried out within the framework of the EUROfusion Consortium and has received funding from the Euratom research and training programme 2014-2018 under grant agreement No 633053. It was supported also by STCU Project No 6058. The views and opinions expressed herein do not necessarily reflect those of the European Commission.

References

[1] ZWEBEN, S., et al, Nucl. Fusion **40** (2000) 91
[2] FASOLI, A., et al., Nucl. Fusion **47** (2007) S264–S284
[3] KIPTILY V.G et al, Nucl.Fusion **65** (2009) 065030
[4] KURKI-SUONIO, T., et al., Nucl. Fusion **49** (2009) 095001
[5] SHINOHARA, K., et al., Nucl. Fusion **51** (2011) 063028
[6] BARANOV, Yu., EPS 2010, paper P5.141
[7] YAVORSKIJ, V., et al., EPS 2011, paper P4.029
[8] GOLOBOROD'KO, V., YAVORSKIJ, V., Nucl. Fusion **29** (1989) 1025
[9] YAVORSKIJ., V.A. et al., Nucl. Fusion **43** (2003) 1077
[10] YAVORSKIJ., V.A. et al., Nucl. Fusion **38**, No. 10 (1998) 1565
[11] PUTVINSKII S.V., "Alpha Particles in Tokamaks", in Rev. of Plasma Physics edited by B.B. Kadomtsev, vol. 18, Consultant Bureau, NY, 1993.
[12] YAVORSKIJ, V., et al., EPS 2012, paper P1.144
[13] YAVORSKIJ, V.A. et al., J Fusion Energy **34** DOI 10.1007/s10894-015-9862-2
[14] HUBA, J.D., NRL Plasma Formulary, Washington, DC 20375-5320, 2002.
[15] YAVORSKIJ, V., et al., Physics of Plasmas **6** (1999) 3853
[16] BELIKOV, V.S., et al., Sov. J. Plasma Phys., **3** (1977) 104

Appendix 1 Fokker-Planck equation for confined ions in $X \equiv \{\mathbf{c}, \vartheta\} = \{V, \xi_m, R_m, \vartheta\}$

To get an explicit expression for $\hat{L}_{\mathbf{x}}$ in $(\mathbf{c}, \vartheta)$ variables we start from the Eulerian representation of drift Fokker-Planck equation with

$$L_{\mathbf{x}} \equiv L_{\mathbf{V}} = \left(\sqrt{g_{\mathbf{V}}}\right)^{-1} \sum_{ij=1,2} \partial_{V^i} \sqrt{g_{\mathbf{V}}} \left(d^i_{\mathbf{V}} - D^{ij}_{\mathbf{V}} \partial_{V^j}\right) f\,, \tag{A1.1}$$

describing collisional relaxation of fast ions on the background plasma. Supposing $V^1=V$ and $V^2=V_{\|}/V=\xi$ we can use well known expressions [14] for transport coefficients of energetic ions of (A1.1) with $d^1_{\mathbf{V}}$ - the slowing down, $d^2_{\mathbf{V}} \equiv 0$, $D^{11}_{\mathbf{V}}$ - diffusion in energy and $D^{22}_{\mathbf{V}}$ - pitch-angle scattering. At a first step we express $L_{\mathbf{V}}$ in terms of new variables $X \equiv \{\mathbf{c}, r\} = \{V, \xi_m, R_m, r\}$ with r the flux surface radius. As a result we obtain

$$L_{\mathbf{cr}} = \left(\sqrt{g_{\mathbf{cr}}}\right)^{-1} \sum_{ij=1,2,3} \partial_{c^i} \sqrt{g_{\mathbf{cr}}} \left(d^i_{\mathbf{cr}} - D^{ij}_{\mathbf{cr}} \partial_{c^j}\right) f\,, \tag{A1.2}$$

where

$$\begin{aligned}
&d^1_{\mathbf{cr}} = d^1_{\mathbf{V}}, \quad d^2_{\mathbf{cr}} = d^1_{\mathbf{V}} \partial_V \xi_m, \quad d^3_{\mathbf{cr}} = d^1_{\mathbf{V}} \partial_V R_m \\
&D^{11}_{\mathbf{cr}} = D^{11}_{\mathbf{V}}, \quad D^{22}_{\mathbf{cr}} = D^{11}_{\mathbf{V}} \left(\partial_V \xi_m\right)^2 + D^{22}_{\mathbf{V}} \left(\partial_\xi \xi_m\right)^2, \quad D^{33}_{\mathbf{cr}} = D^{11}_{\mathbf{V}} \left(\partial_V R_m\right)^2 + D^{22}_{\mathbf{V}} \left(\partial_\xi R_m\right)^2. \\
&D^{12}_{\mathbf{cr}} = D^{11}_{\mathbf{V}} \partial_V \xi_m, \quad D^{13}_{\mathbf{cr}} = D^{11}_{\mathbf{V}} \partial_V R_m, \quad D^{23}_{\mathbf{cr}} = D^{11}_{\mathbf{V}} \partial_V \xi_m \partial_V R_m + D^{22}_{\mathbf{V}} \partial_\xi \xi_m \partial_\xi R_m
\end{aligned} \tag{A1.3}$$

Using the relationships between Eulerian variable $\{\mathbf{r}, \mathbf{V}\}$ and new Lagrangian variables $\{r, \mathbf{c}\}$ following from the constants of motion in drift approximation, i.e.

$$\xi b^{-1} = \frac{\Psi(r) - P_{\mathbf{c}}}{\rho}, \quad b^{-1} = \frac{\lambda_{\mathbf{c}}}{2} + \sqrt{\frac{\lambda_{\mathbf{c}}^2}{4} + \left(\frac{P_{\mathbf{c}} - \Psi}{\rho}\right)^2}\,. \tag{A1.4}$$

Here Ψ(r) is the poloidal magnetic flux, $b=B/B_{\mathrm{c}}$, B_{c} is the magnetic field at the plasma centre ($R=R_{\mathrm{c}}$, $Z=Z_{\mathrm{eq}}$), $P_{\mathbf{c}} = \Psi(r_m) - \rho \xi_m b_m^{-1}$ and $\lambda_{\mathbf{c}} = R_m\left(1-\xi_m^2\right) R_{\mathrm{c}}^{-1}$ are correspondingly toroidal canonical momentum and normalised magnetic moment, r_{m} is the radius of flux surface at $R=R_{\mathrm{m}}$, $\mathrm{Z}=\mathrm{Z}_{\mathrm{eq}}$. Relationships (A1.4) allow getting the explicit expressions for $\partial_\xi R_m$, $\partial_V R_m$, $\partial_\xi \xi_m$, $\partial_V \xi_m$ and for Jacobian $\sqrt{g_{\mathbf{cr}}}$ -

$$\begin{aligned}
&\partial_\xi R_m = 2\frac{\xi_m - \xi}{b\kappa}, \quad \partial_V R_m = 2\frac{\xi_m}{V\kappa}\left(\frac{\xi_m}{b_m} - \frac{\xi}{b}\right), \quad \kappa = \left(1 + \xi_m^2 - 2\frac{\xi_m}{\delta}\right)\partial_{R_m} b_m^{-1} \\
&\partial_\xi \xi_m = \frac{b_m}{\xi_m}\frac{\xi}{b} + \frac{\xi_m - \xi}{b\xi_m \eta}, \quad \partial_V \xi_m = \frac{1}{V\eta}\left(\frac{\xi_m}{b_m} - \frac{\xi}{b}\right), \quad \eta = \left(1 + \xi_m^2 - 2\frac{\xi_m}{\delta}\right)\left(1+\xi_m^2\right)^{-1} b_m^{-1}. \\
&\sqrt{g_{V\xi_m R_m r}} = \frac{YR^2V^2 b_m^{-1}\kappa}{\left(1+\xi^2\right) b^{-1} \partial_\chi b^{-1}}
\end{aligned} \tag{A1.5}$$

In (A1.5) YR^2 is the Jacobian of transformation from cylindrical coordinate R, Z to flux coordinate r, χ [15]. It can be shown that $\sqrt{g_{\mathbf{cr}}}\dot{r} = \Omega(\mathbf{c})$, i.e. is a constant of motion with

$$\Omega(\mathbf{c}) = \sigma_J \rho R_c V^3 b_m^{-1} \kappa / 2 . \qquad \text{(A1.6)}$$

In (A1.6) σ_J is a sign of toroidal current in plasma (see Fig. 5). Introducing the poloidal variable ϑ determined by the relationship (5) we express $L_{\mathbf{x}}$ in terms of new variables $\{\mathbf{c}, \vartheta\} \equiv \{V, \xi_m, R_m, \vartheta\}$ and get the following Fokker-Planck equation

$$\begin{aligned}
&\Omega(\mathbf{c})\frac{\partial}{\partial \vartheta} f = L_{\mathbf{c}} f + L_{\vartheta} f + \sqrt{g_{\mathbf{c}\vartheta}} S(\mathbf{c}, \vartheta) \\
&L_{\mathbf{c}} = \sum_{ij=1,2,3} \partial_{c^i} \sqrt{g_{\mathbf{c}\vartheta}} \left(d^i_{\mathbf{c}\vartheta} - D^{ij}_{\mathbf{c}\vartheta} \partial_{c^j} \right) \\
&L_{\vartheta} = \partial_{\vartheta} \sqrt{g_{\mathbf{c}\vartheta}} \left(d^4_{\mathbf{c}\vartheta} - \sum_{i=1,2,3} D^{4i}_{\mathbf{c}\vartheta} \partial_{c^i} \right) - \sum_{i=1,2,3} \left(\partial_{c^i} \sqrt{g_{\mathbf{c}\vartheta}} D^{i4}_{\mathbf{c}\vartheta} \partial_{\vartheta} + \partial_{\vartheta} \sqrt{g_{\mathbf{c}\vartheta}} D^{44}_{\mathbf{c}\vartheta} \partial_{\vartheta} \right)
\end{aligned} . \qquad \text{(A1.7)}$$

with

$$\begin{aligned}
&d^i_{\mathbf{c}\vartheta} = d^i_{\mathbf{cr}}, \quad D^{ij}_{\mathbf{c}\vartheta} = D^{ij}_{\mathbf{cr}} \quad \text{for} \quad i, j \neq 4 \\
&d^4_{\mathbf{c}\vartheta} = d^1_{\mathbf{cr}} \partial_V \vartheta + d^2_{\mathbf{cr}} \partial_{\xi_m} \vartheta + d^3_{\mathbf{cr}} \partial_{R_m} \vartheta \\
&D^{41}_{\mathbf{c}\vartheta} = D^{11}_{\mathbf{cr}} \partial_V \vartheta + D^{21}_{\mathbf{cr}} \partial_{\xi_m} \vartheta + D^{31}_{\mathbf{cr}} \partial_{R_m} \vartheta \\
&D^{42}_{\mathbf{c}\vartheta} = D^{12}_{\mathbf{cr}} \partial_V \vartheta + D^{22}_{\mathbf{cr}} \partial_{\xi_m} \vartheta + D^{32}_{\mathbf{cr}} \partial_{R_m} \vartheta \\
&D^{43}_{\mathbf{c}\vartheta} = D^{13}_{\mathbf{cr}} \partial_V \vartheta + D^{32}_{\mathbf{cr}} \partial_{\xi_m} \vartheta + D^{33}_{\mathbf{cr}} \partial_{R_m} \vartheta \\
&\sqrt{g_{\mathbf{c}\vartheta}} = \partial_r \vartheta \sqrt{g_{\mathbf{cr}}}, \quad \Omega(\mathbf{c}) = \sqrt{g_{\mathbf{c}\vartheta}} \dot{\vartheta}
\end{aligned} . \qquad \text{(A1.8)}$$

Accounting for relationship

$$\sin^2 \frac{\vartheta}{2} = \frac{r_m(R_{\mathrm{m}}) - r}{r_m(R_{\mathrm{m}}) - r_{\min}(V, \xi_m, R_{\mathrm{m}})} \qquad \text{(A1.9)}$$

derivatives $\partial_{\mathbf{cr}} \vartheta$ in (A1.8) can be represented as

$$\begin{aligned}
&\partial_r \vartheta = -\frac{2}{\Delta \sin \vartheta} \\
&\partial_{R_m} \vartheta = \frac{1}{\Delta} \partial_{R_{\mathrm{m}}} r_{\mathrm{m}} \tan^{-1} \frac{\vartheta}{2} + \frac{1}{\Delta} \tan \frac{\vartheta}{2} \partial_{R_{\mathrm{m}}} r_{\min} \\
&\partial_{\xi_m} \vartheta = \frac{1}{\Delta} \tan \frac{\vartheta}{2} \partial_{\xi_{\mathrm{m}}} r_{\min}, \quad \partial_V \vartheta = \frac{1}{\Delta} \tan \frac{\vartheta}{2} \partial_V r_{\min}
\end{aligned} . \qquad \text{(A1.10)}$$

Due to weak collision rates as compared to bounce frequencies the distribution function of fast ions, $f(\mathbf{c},\vartheta)$, can be represented as a superposition of the dominant part, $f_0(\mathbf{c})$, which is independent on angular coordinate and of a small oscillating part, $f_1(\mathbf{c},\vartheta)$,

$$f = f_0(\mathbf{c}) + f_1(\mathbf{c},\vartheta), \quad f_1 \propto O(\delta f_0), \quad \delta = \frac{\max\{\nu_s, A^2\nu_\perp\}}{|\dot{r}/r|} \simeq \frac{\max\{\nu_s, A^2\nu_\perp\}}{V_d/r} << 1. \quad \text{(A1.11)}$$

Using (A9) we arrive at the following equation for f_0

$$\langle L_{\mathbf{c}} \rangle f_0 + \left\langle \sqrt{g_{\mathbf{c}\vartheta}} S(\mathbf{c},\vartheta) \right\rangle = 0, \quad \langle ... \rangle = \int_0^{2\pi} (...) d\vartheta. \quad \text{(A1.12)}$$

Finally the $f_1(\mathbf{c},\vartheta)$ can be represented as

$$\begin{aligned} &\Omega(\mathbf{c}) f_1 = \langle L_{\mathbf{c}} \rangle_\vartheta f_0 + \langle L_\vartheta \rangle_\vartheta f_0 + \left\langle \sqrt{g_{\mathbf{c}\vartheta}} S(\mathbf{c},\vartheta) \right\rangle_\vartheta \\ &\langle L_\vartheta \rangle_\vartheta = \sum_{i=1,2,3} \left\langle \sqrt{g_{\vartheta\mathbf{c}}} \left(d^4_{\vartheta\mathbf{c}} - D^{4i}_{\vartheta\mathbf{c}} \partial_{c^i} \right) \right\rangle_\vartheta, \quad \langle ... \rangle_\vartheta = \int_0^{\vartheta} (...) d\vartheta \end{aligned}. \quad \text{(A1.13)}$$

It should be noted that $D^{44}_{\vartheta\mathbf{c}}$ does not contribute to $f_1(\mathbf{c},\vartheta)$.

Appendix 2 Fokker-Planck equation for lost ions in coordinates $\hat{X} \equiv \{\mathbf{c}_l, \hat{\vartheta}\} = \{V, \xi_l, Z_l, \hat{\vartheta}\}$

To get an expression for $L_{\mathbf{x}}$ in $\{\mathbf{c}_l, \hat{\vartheta}\}$ variables we follow the procedure of **Appendix 1**. Using the following relationships of Eulerian coordinates with New Lagrangian coordinates $\{\mathbf{c}_l, \hat{\vartheta}\} = \{V, \xi_l, Z_l, \hat{\vartheta}\}$ given by

$$\begin{aligned} &\xi h = \frac{\Psi(r) - \Psi(r_{gl})}{\rho} + \frac{\xi_l R_{gl}(V,\xi_l,Z_l)}{R_c}, \quad h = \frac{R}{R_c}, \quad r_{gl} = r(R_{gl}, Z_{gl}) \\ &h = \frac{\lambda_{\mathbf{c}}}{2} + \sqrt{\frac{\lambda_{\mathbf{c}}^2}{4} + \left(\frac{\Psi - \Psi_{gl}}{\rho} + \frac{\xi_l R_{gl}}{R_c} \right)^2} = \frac{\lambda_{\mathbf{c}}}{2} + \sqrt{\frac{\lambda_{\mathbf{c}}^2}{4} + \left(\frac{P_{\mathbf{c}} - \Psi}{\rho} \right)^2} \\ &\lambda_{\mathbf{c}} = (1 - \xi_l^2) \frac{R_{gl}}{R_c}, \quad P_{\mathbf{c}} = \Psi(r_{gl}) - \rho \frac{\xi_l R_{gl}}{R_c} \\ &r = r_{gl}(R_{gl}, Z_{gl}) \cos^2 \frac{\vartheta}{2} + r_{\min}(V, \xi_l, Z_l) \sin^2 \frac{\hat{\vartheta}}{2} \end{aligned}. \quad \text{(A2.1)}$$

Using (A2.1) we arrive at the following FP equation for lost ions

$$\hat{\Omega}(\mathbf{c}_l)\partial_{\hat{\vartheta}} f = L_{\mathbf{c}_l} f + L_{\hat{\vartheta}} f$$
$$L_{\mathbf{c}_l} = \sum_{ij=1,2,3} \partial_{c^i} \sqrt{g_{\mathbf{c}_l\hat{\vartheta}}} \left(d^i_{\mathbf{c}_l\hat{\vartheta}} - D^{ij}_{\mathbf{c}_l\hat{\vartheta}} \partial_{c^j} \right) \quad . \qquad \text{(A2.2)}$$
$$L_{\hat{\vartheta}} = \partial_{\hat{\vartheta}} \sqrt{g_{\mathbf{c}_l\hat{\vartheta}}} \left(d^4_{\mathbf{c}_l\hat{\vartheta}} - \sum_{i=1,2,3} D^{4i}_{\mathbf{c}_l\hat{\vartheta}} \partial_{c^i} \right) - \sum_{i=1,2,3} \left(\partial_{c^i} \sqrt{g_{\mathbf{c}_l\hat{\vartheta}}} D^{i4}_{\mathbf{c}_l\hat{\vartheta}} \partial_{\hat{\vartheta}} + \partial_{\hat{\vartheta}} \sqrt{g_{\mathbf{c}_l\hat{\vartheta}}} D^{44}_{\mathbf{c}_l\hat{\vartheta}} \partial_{\hat{\vartheta}} \right)$$

In (A2.2)

$$\sqrt{g_{\hat{\vartheta}V\xi_l Z_l}} = -V^2 Y R^2 \frac{\mathrm{K}(\mathbf{c}_l)}{2\rho(1+\xi^2)h\partial_\chi h} \Delta \sin\hat{\vartheta}, \quad \sqrt{g_{\hat{\vartheta}V\xi_l Z_l}}\dot{\vartheta} \equiv \sigma_J R_c V^3 \frac{\mathrm{K}(\mathbf{c}_l)}{2} = \hat{\Omega}(\mathbf{c}_l)$$

$$\mathrm{K}(\mathbf{c}_l) = \left(\frac{\lambda}{R_{gl}} \partial_{\xi_l} R_{gl} - \frac{2\xi_l R_{gl}}{R_c} \right) \partial_{Z_{gl}} \Psi(R_{gl}, Z_{gl}) \hat{H}(R_{gl}, Z_l) + \frac{\rho_c}{R_c} \frac{R_{gl}}{R_c} \left(1 + \xi_l^2 - \frac{2\xi_l}{\delta_l} \right) \partial_{Z_l} R_{gl}$$
$$\delta_l = \frac{\rho_c}{R_c \partial_{R_{gl}} \Psi\left[R_{gl}, Z_{gl}(Z_l, R_{gl}) \right]}, \hat{H} = 1 + W''(Z_l)\left[W(Z_l) - R_{gl} \right] + W'^2(Z_l), \qquad \text{(A2.3)}$$
$$\partial_{R_{gl}} \Psi\left[R_{gl}, Z_{gl}(Z_l, R_{gl}) \right] \equiv \partial_R \Psi(R,Z)\big|_{R=R_{gl}, Z=Z_l} - W'(Z_l)\partial_Z \Psi(R,Z)\big|_{R=R_{gl}, Z=Z_l},$$
$$\partial_{Z_{gl}} \Psi(R_{gl}, Z_{gl}) = \partial_Z \Psi(R,Z)\big|_{R=R_{gl}, Z=Z_{gl}}, \rho_c = \frac{V}{\omega_c}$$

Due to condition (8) equation (A2.2) can written as

$$\hat{\Omega}(\mathbf{c}_l)\partial_{\hat{\vartheta}} f = \partial_{Z_l} \sqrt{g_{\mathbf{c}_l\hat{\vartheta}}} \left(d^3_{\mathbf{c}_l\hat{\vartheta}} - D^{33}_{\mathbf{c}_l\hat{\vartheta}} \partial_{Z_l} \right) f \qquad \text{(A2.4)}$$

with the following transport coefficients

$$d^3_{\mathbf{c}_l\hat{\vartheta}} = d^1_{\mathbf{V}} \partial_V Z_l$$
$$D^{33}_{\mathbf{c}_l\hat{\vartheta}} = D^{11}_{\mathbf{V}} (\partial_V Z_l)^2 + D^{22}_{\mathbf{V}} (\partial_\xi Z_l)^2 \quad . \qquad \text{(A2.5)}$$

In (A2.5)

$$\partial_V Z_l = \frac{\rho R \xi}{V R_c} \partial_{\xi_l} \lambda_{\mathbf{c}_l} \mathrm{K}^{-1}(\mathbf{c}_l)$$
$$\partial_\xi Z_l = \frac{\rho}{R_c} \frac{R}{R_c} \left[2R_{gl}(\xi_l - \xi) - \left(1 - \xi_l^2 + 2\xi_l \xi - \frac{2\xi}{\delta_l} \right) \partial_{\xi_l} R_{gl} \right] \mathrm{K}^{-1}(\mathbf{c}_l) \quad .$$

Figures

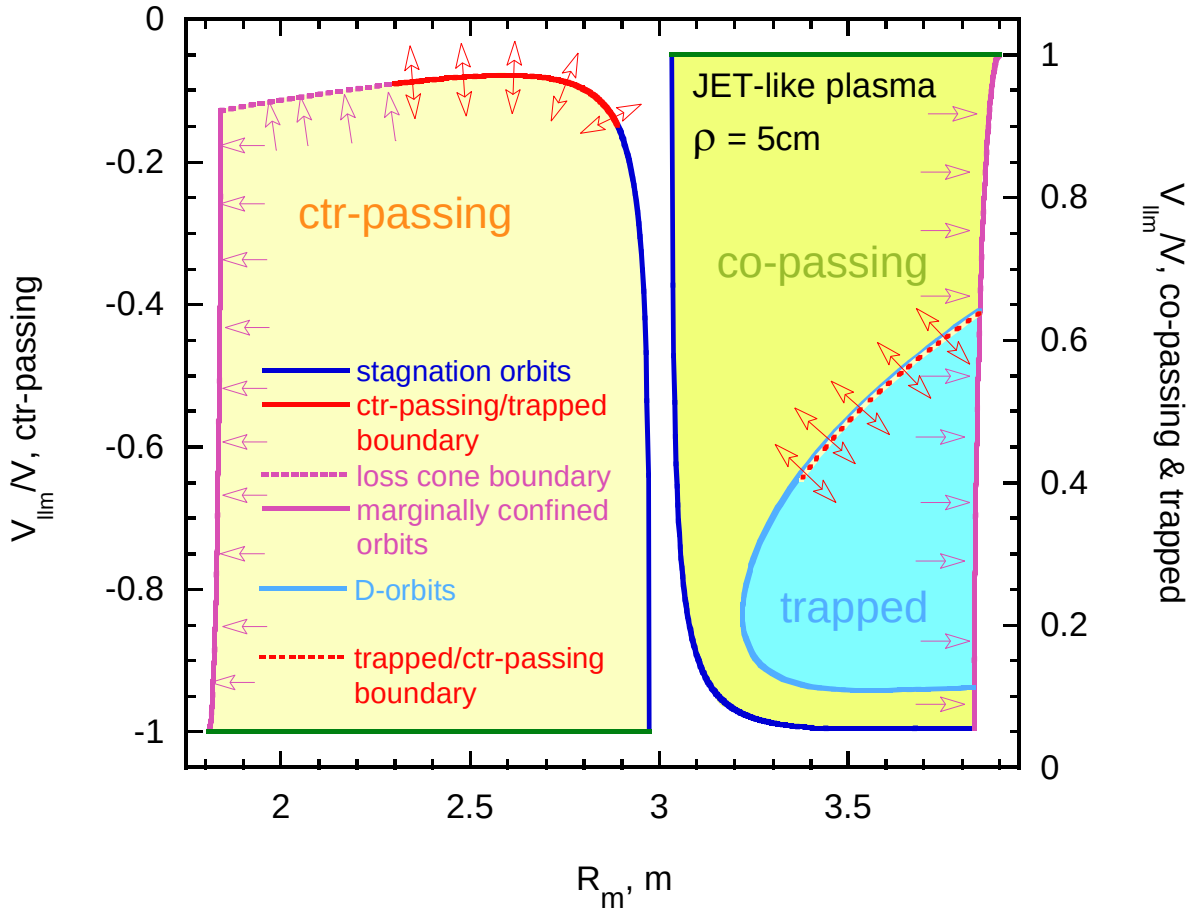

Fig. 1: Confinement domains of counter-passing (left) and co-passing and trapped (right) fast ions with full gyro-radius ρ =5cm in constant-of-motion variables R_m and pitch-angle cosine $\xi_m=V_{\|m}/V$ confined in JET-like plasma ($q_a/q_0=5/1$, Shafranov shift $\Delta_0=0.15$m and elongation $k=1.7$). Here $\rho=(2mE/m)^{1/2}c/(eB_c)$ – gyro-radius at the plasma centre ($R_c=2.86$m).

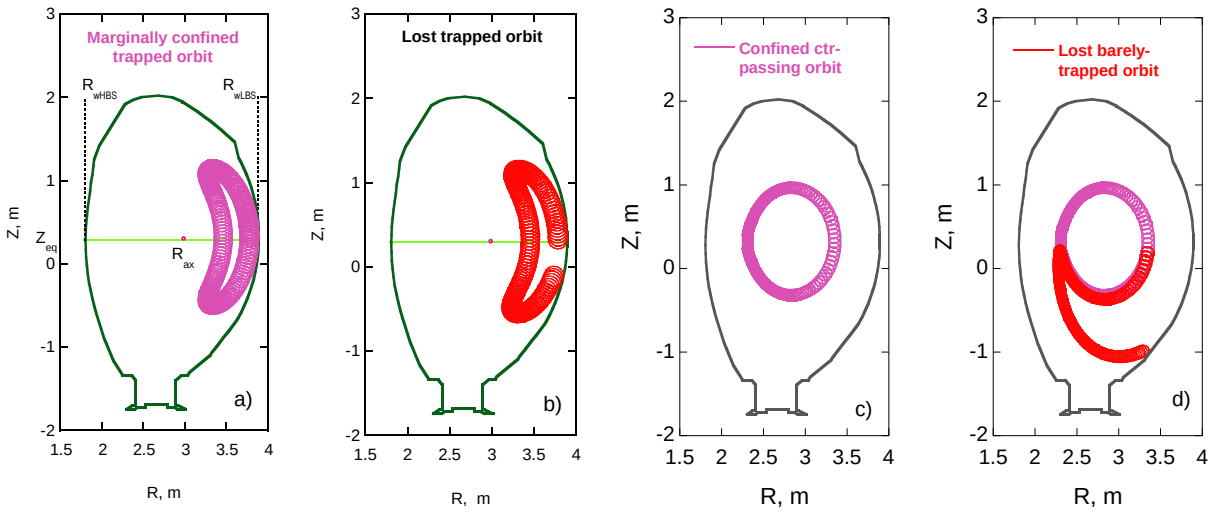

Fig. 2: Distinctive orbits of fast ions lost a result of radial diffusion – b) and via scattering into a loss cone – d). Shown in violate are unperturbed marginally confined trapped – a) and confined ctr-passing – c), d) orbits.

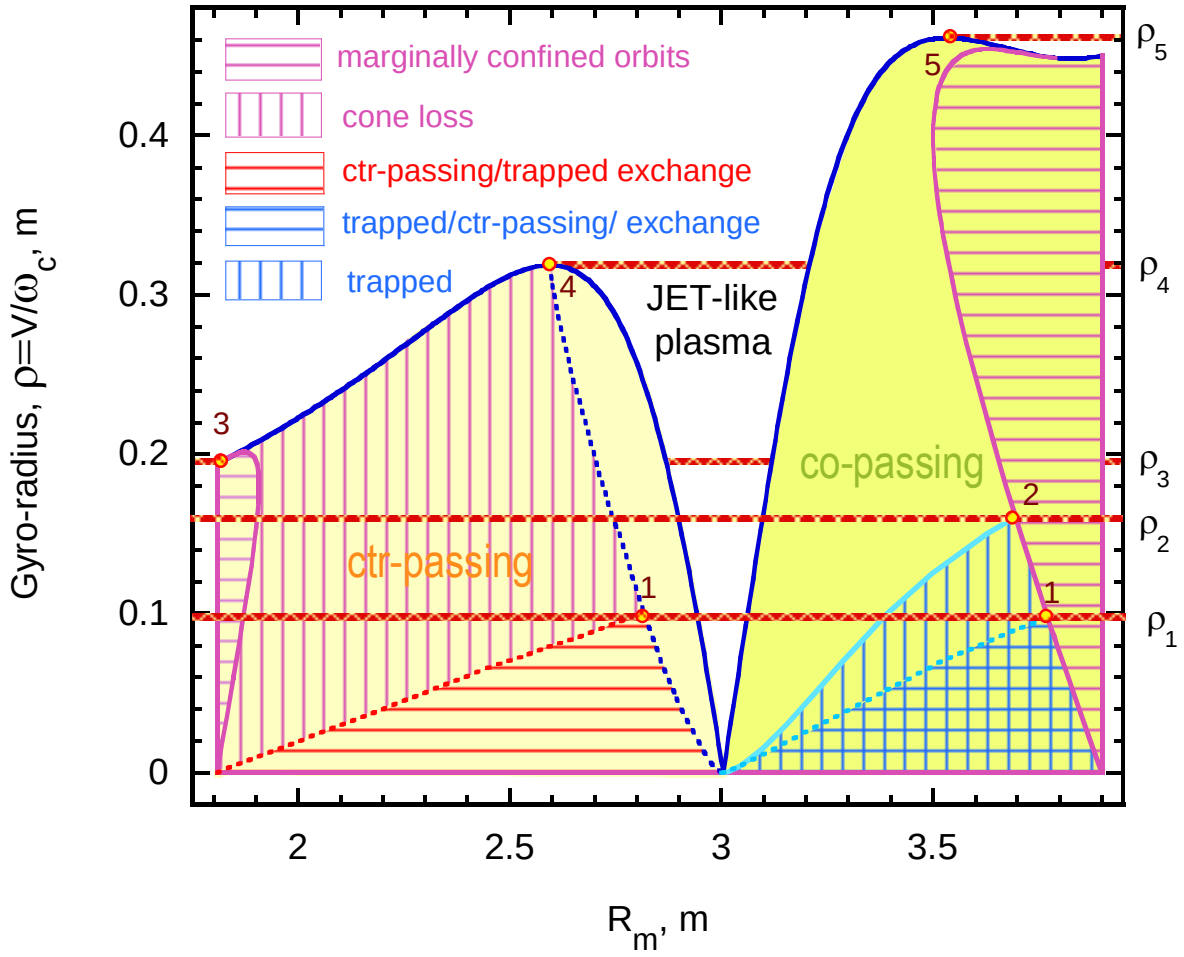

Fig. 3: Confinement domains of counter-passing (left) and co-passing and trapped (right) fast ions in constant-of-motion variables R_m, ρ confined in JET-like plasma (q_a/q_0=5/1, Shafranov shift Δ_0=0.15m and elongation k=1.7). Here $\rho = (2mE/m)^{1/2}c/(eB_c)$ – full gyro-radius at the plasma centre (R_c=2.86m). ρ_1, ρ_2, …, ρ_5 are characteristic values of gyro-radius separating energy ranges with qualitatively different orbit topology of confined fast ions and with different loss mechanisms.

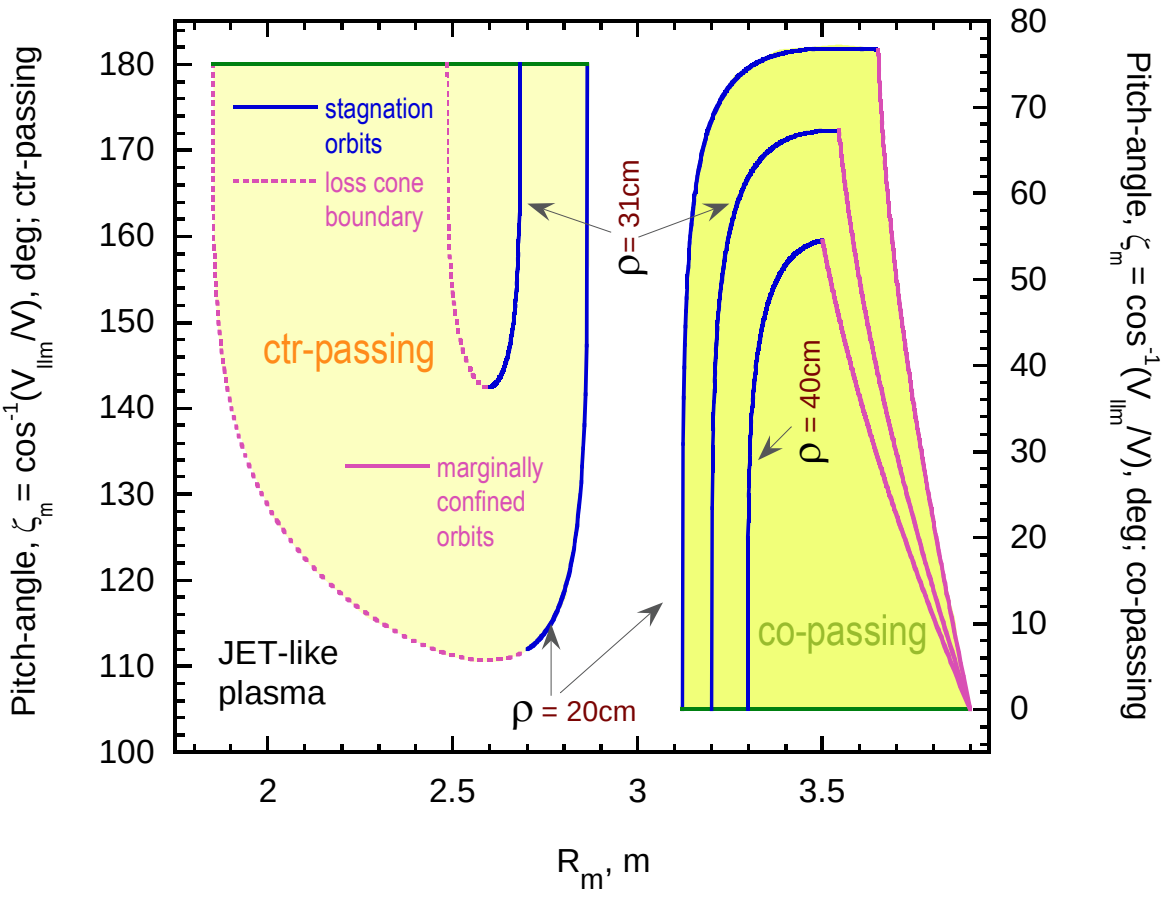

Fig. 4: Confinement domains of counter-passing (left) and co-passing (right) fast ions with full gyro-radii ρ =20cm, 31cm and 40cm in constant-of-motion variables R_m, ξ_m confined in JET-like plasma (q_a/q_0=5/1, Shafranov shift Δ_0=0.15m and elongation k=1.7). Here $\rho = (2mE/m)^{1/2}c/(eB_c)$ – gyro-radius at the plasma centre (R_c=2.86m).

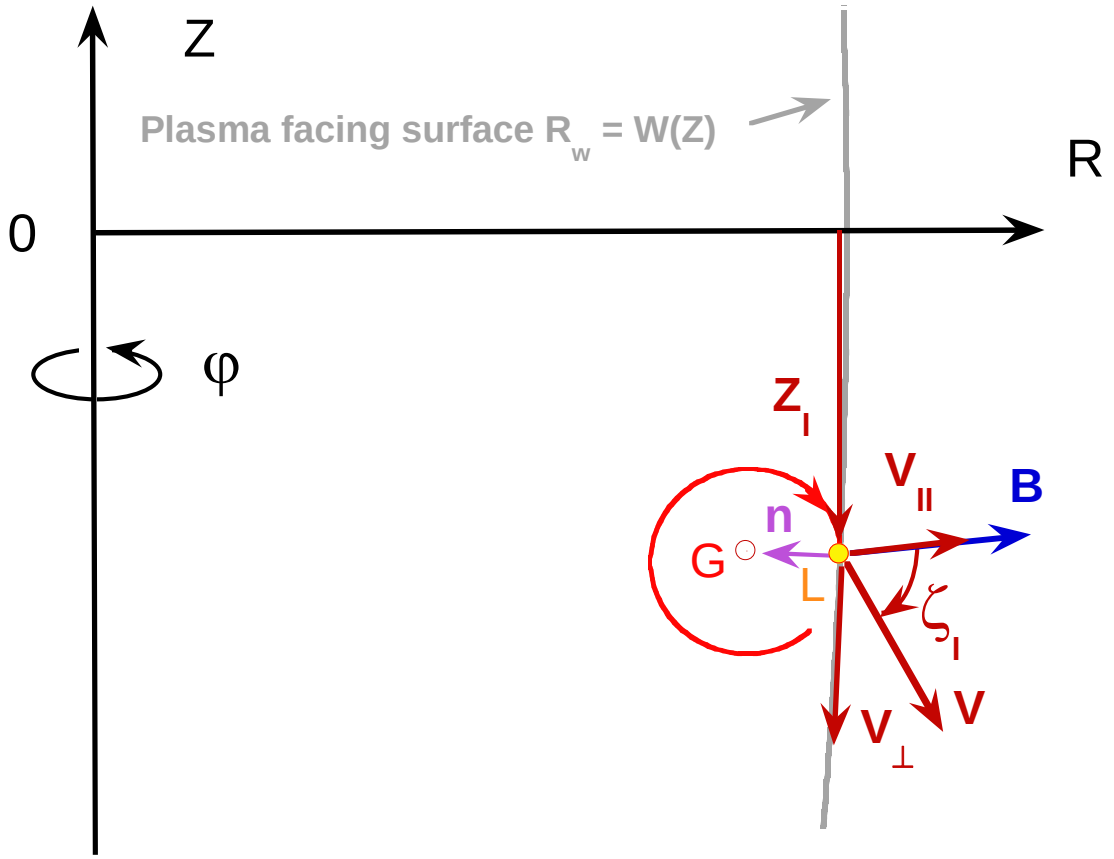

Fig. 5: Constant-of-motion variables of lost ions. Here Z_l and ζ_l are values of Z coordinate and pitch-angle at the point L, where ion hits the PFS; G is the guiding centre position at the moment when the ion reaches the point L; n is the normal to PFS at the point L.

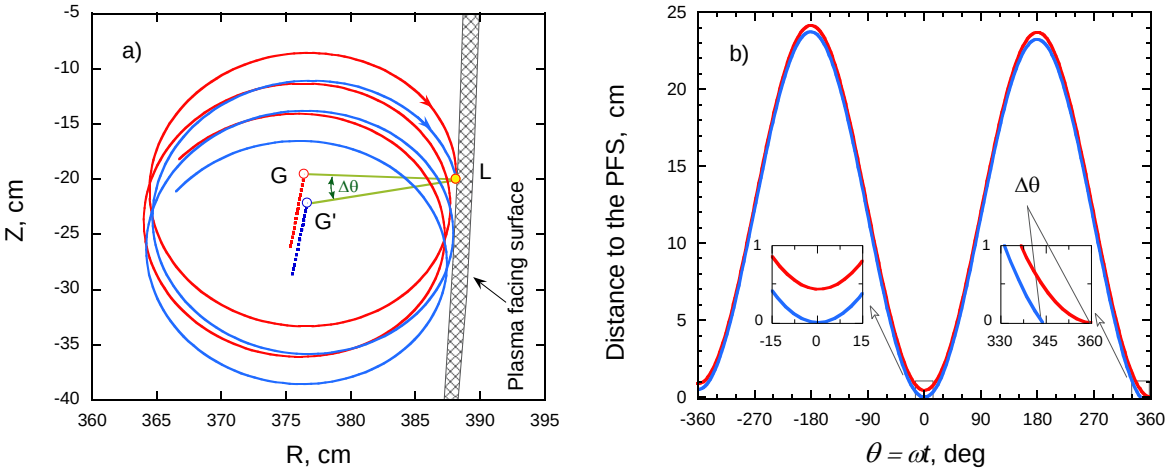

Fig. 6: (a) - Typical orbits of fast ions escaping to the plasma facing surface at point $L(R_l,Z_l)$ with the same pitch-angle ζ_l but with minimum (red) and maximum (blue) values of the normal to the PFS velocity. (——, ——)- full orbits, (---,---) - guiding centre orbits. Points $G(R_g,Z_g)$ and $G'(R'_g,Z'_g)$ denote the guiding centre positions at the moment when ion hits the PFS. (b) – Distance between the ion and the plasma facing surface as a function of gyro phase $\theta = \omega t$. $\theta = 0°$ corresponds to the closest approach to PFS during the gyro period prior the ion loss.

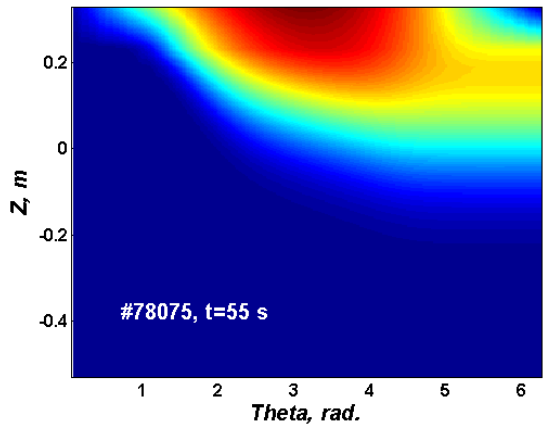

Fig. 7: Fast ion distribution function of co-circulating lost deuterons with E = 130 keV and ξ_l=0.5 vs polidal angular variable $\hat{\vartheta}$ and poloidal coordinate Z_l at the first wall.

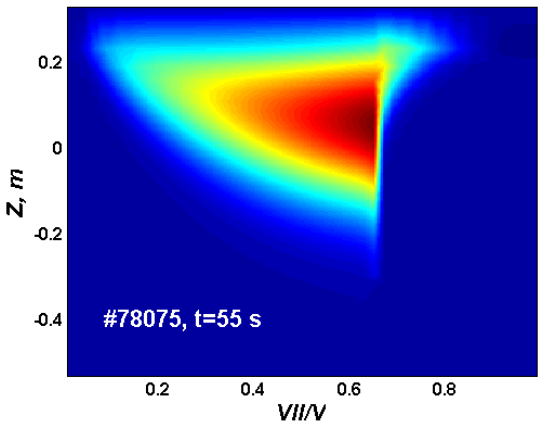

Fig. 8: Contours of the convection-diffusion collisional flux of trapped and co-passing beam deuterons in the plane spanned by the pitch angle cosine ξ and poloidal coordinate Z at the first wall.